Journal of Population Therapeutics & Clinical Pharmacology

RESEARCH ARTICLE
DOI: 10.53555/jptcp.v31i4.5374

SYNTHESIS AND CHARACTERIZATION OF ZINC NANOPARTICLES USING THERMOSETTING RESINS

Jyoti Chaudhary[1], Vipin Khoker[2*], Giriraj Tailor[3]

[1,2 *]Department of Chemistry, M.L.S. University, Udaipur, Rajasthan, India, 313001
[3]Department of Chemistry, Mewar University, Gangrar, Chittorgarh, Rajasthan, India, 312901
Email- khokervipin@mlsu.ac.in

*** Corresponding Author:** Vipin Khoker
*Department of Chemistry, M.L.S. University, Udaipur, Rajasthan, India, 313001

Abstract
In this study, urea-formaldehyde nanoparticles doped with zinc and measuring an average of 26.10 nm in size were created using a straightforward chemical process. FT-IR and NMR spectroscopy have verified that the zinc polymer metal complex has formed successfully. X-ray diffraction, energy dispersive X-ray (EDX), and scanning electron microscopy (SEM) were used to measure the concentrations of these nanoparticles. XRD. Zinc salts and thermosetting polymer were used as precursors to create Zn NPs. After 30 minutes of calcination at 800 °C, Zn NPs were produced. Synthesized nanoparticles have a spherical form, according to a SEM investigation. The Zn NPs that are generated are crystalline, according to XRD examination..

1. Introduction

A high-performance resin known as urea-formaldehyde (PF) is created when formaldehyde and urea copolymerize. It is extensively used in the industrial sector for plastics, adhesives, and impregnating resins. UF resin has strong mechanical, thermal, and weather stability, among other excellent qualities [1]. UF resins can be used in impregnating resins or adhesives, but their application is limited by their greater curing temperature need and lower curing rate when compared to other thermosetting adhesives [2, 3]. Nanoparticles (NPs) possess distinct characteristics due to their small size and high surface to volume ratio. The application of these particles is expanding across numerous domains. Over the past three decades, there has been a surge in research interest in nanoparticles and their size-dependent features [4-6]. Because of its beneficial electrical, optical, dermatological, and antibacterial qualities, zinc nanoparticles are being used extensively in many different disciplines [7-9]. The band gap of 3.37 eV in zinc oxide nanoparticles is significant for a number of applications [10–11]. Since zinc has been extracted from dyes and water pollutants in textile effluents, there has been a rise in interest in zinc nanoparticles [12–13]. Zinc nanoparticles (Zn NPs) have potential uses in the pharmacological and biological fields and can be employed as efficient instruments for controlling mosquito larval populations [14].Numerous methods for synthesizing Zinc Nanoparticles (Zn NPs) have been reported in the chemical literature due to their vast array of applications. Chemical procedures such as sol-gel processing, precipitation, electro-deposition, and thermal processes have been reported for preparation [15–18]. Nonetheless, due to its numerous benefits, the thermal breakdown method is frequently chosen over alternative approaches [19–20]. Because this approach uses less expensive chemicals and simpler equipment, production costs are quite low. Furthermore, stable monodispersed products may be produced and a greater number of environmentally suitable

and less harmful components are used. It has been revealed that zinc salt precursors play a significant impact in the surface morphology and characteristics during the nano production of these particles [21]. Therefore, it is crucial to use microscopy techniques to characterize the size, shape, and position of the synthesized Zn NPs. This study describes the synthesis of zinc nanoparticles using a thermal decomposition approach, as well as the characterization of the particles using transmission electron microscopy (TEM), scanning electron microscopy (SEM), and X-ray diffraction. The goal of the study was to validate the utility of the low-cost method for the synthesis of possible high-utility Zn NPs by characterizing the Zn NPs formed by thermal disintegration of the Zn-polymer complex generated in the laboratory using various microscopy techniques.

2. Materials and methods-

The experiment uses only analytical-grade chemicals. We bought zinc chloride (ZnCl2), hydrochloric acid (HCl), formaldehyde (HCHO), urea (CO(NH2)2), and acetic acid (CH3COOH) from Central Drug House Ltd. in India. Every chemical that was obtained from the supplier was used. The entire experiment was conducted with deionized water.

Synthesis of the nanoparticles-

The synthesis was carried out in two steps:

Step 1: Synthesis of Zinc doped Urea-Formaldehyde complex

Step 2: Synthesis of zinc nanoparticle

Step 1: **Synthesis of Zinc doped Urea-Formaldehyde complex**

This three-necked round-bottom flask has a reflux condenser and stirrer, and it can store 1.38 moles of urea, 1.13 moles of formaldehyde solution, and 15 milliliters of glacial acetic acid. The mixture is shaken well and then allowed to cool. The remaining water is removed by progressively raising the temperature to 500C and using a water pump to create a vacuum. This temperature is maintained until the melt sample solidifies and becomes a white solid. The zinc polymer compound is prepared by additional It was mixed in 1N zinc salt solution. Shake the mixture for five minutes. The reaction has an exothermic character. After removing extra metal ions, the dried solid sample was cleaned in distilled water to ensure purity. The reaction scheme show in fig.1

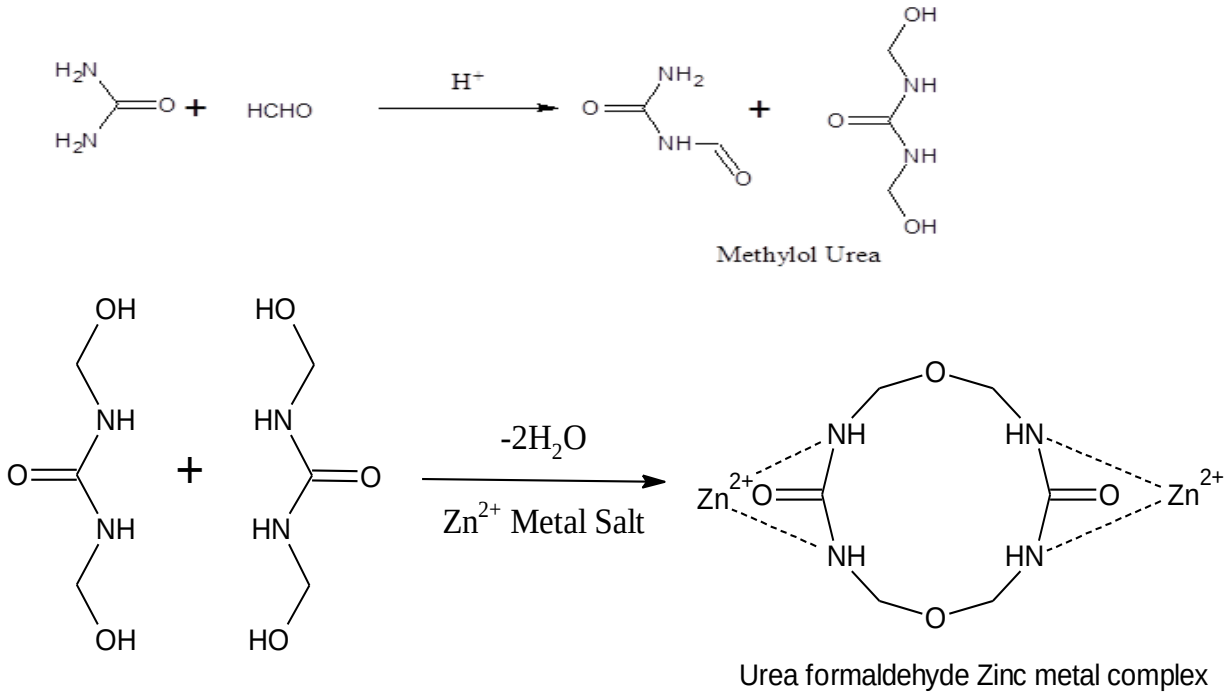

Figure-1 Synthesis Scheme of zinc doped Urea-Formaldehyde complex

Step 2: Synthesis of zinc nanoparticle

Zinc nanoparticles were created by thermal degradation with phenol-formaldehyde resin. The polymer metal composite is allowed to decompose at 8000C for 60 minutes. Fine, black-colored zinc nanoparticles were the result of disintegration.

Purification of zinc nanoparticles: -

Step 1: Elimination of Volatile Impurity: During the decomposition process, a number of volatile impurities were removed, leaving the nanoparticle free of these impurities.

Step 2: Elimination of Metallic Impurities: The nanoparticle was subjected to a 24-hour immersion in 12N hydrochloric acid in order to eliminate any metallic ions. After centrifuging the mixture, distilled water was used to entirely eliminate the hydrochloric acid.

Fourier Transform Infrared spectroscopy (FT-IR) –

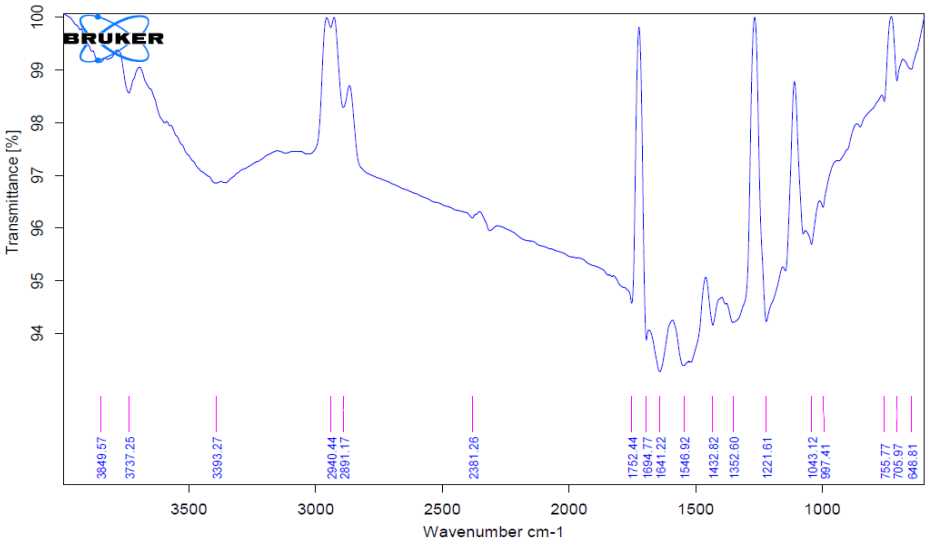

Figure-2 FTIR Spectra of zinc doped Urea – Formaldehyde Complex

Nuclear magnetic resonance spectroscopy:

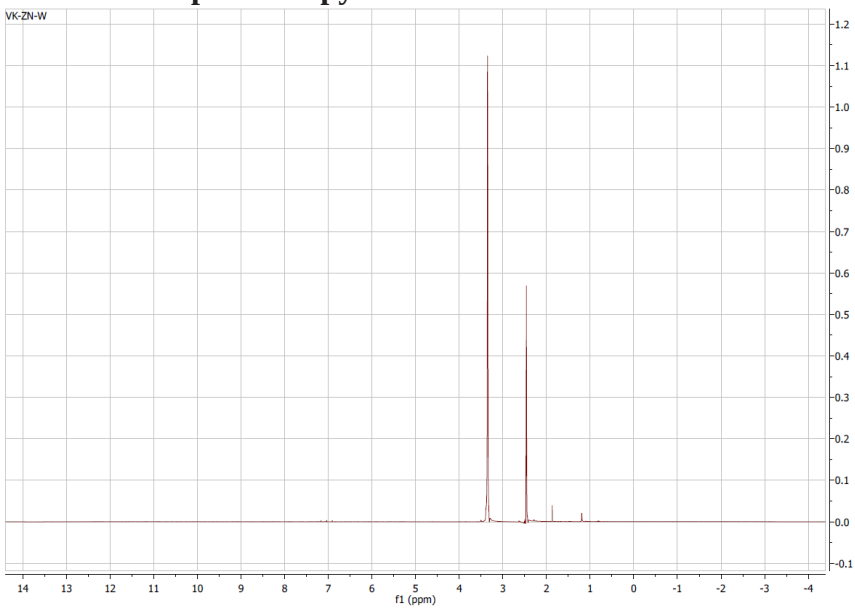

Figure-3 ^{1}HNMR Spectra of zinc doped Urea – Formaldehyde Complex

Scanning Electron Microscopy (SEM):

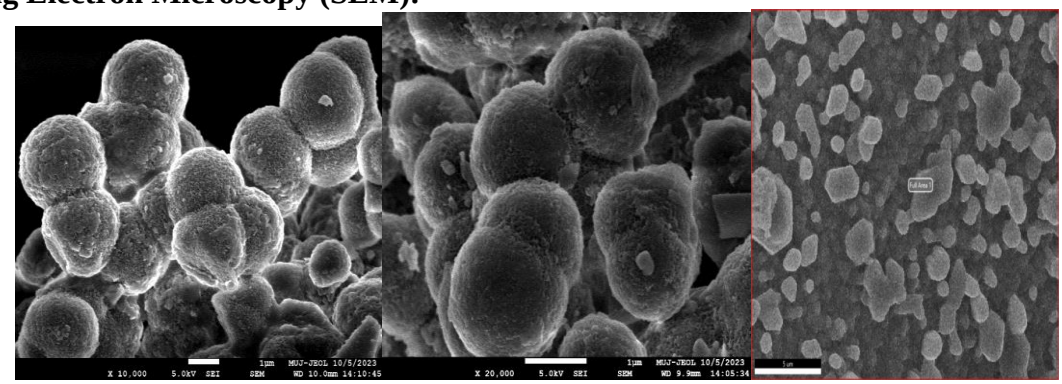

Figure-4 SEM image of zinc nanoparticles usingUrea-formaldehyde resin at (a) 10000 and (b) 20000 magnifications

Energy Dispersive X-Ray (EDX)

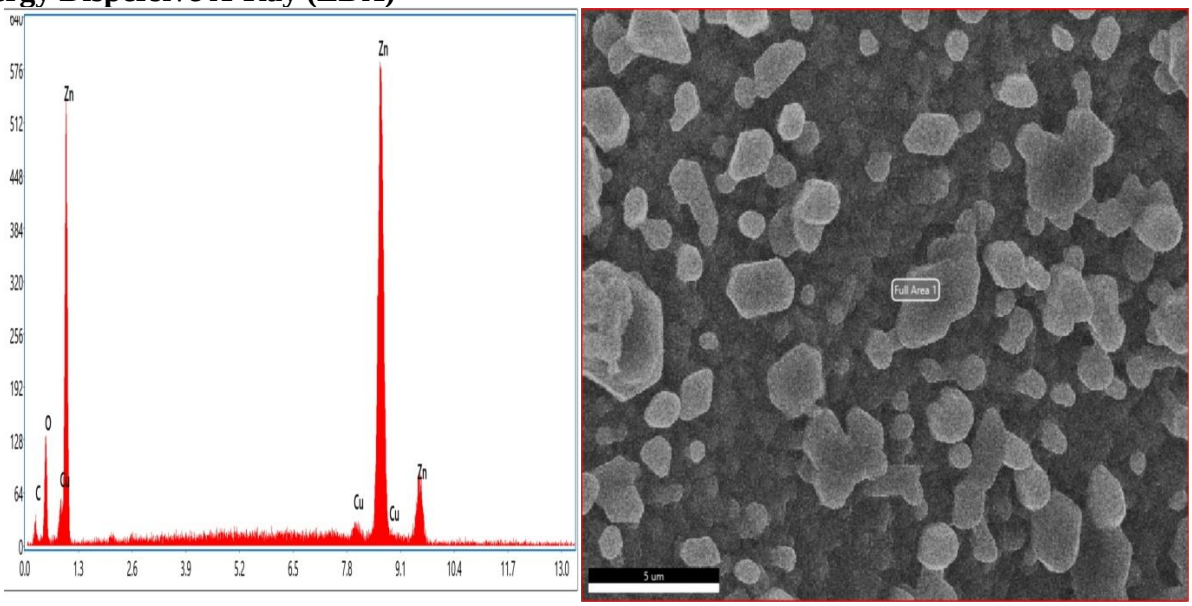

Figure-5 EDX analysis of zinc nanoparticles using Urea-formaldehyde resin

X-ray diffraction (X-RD)

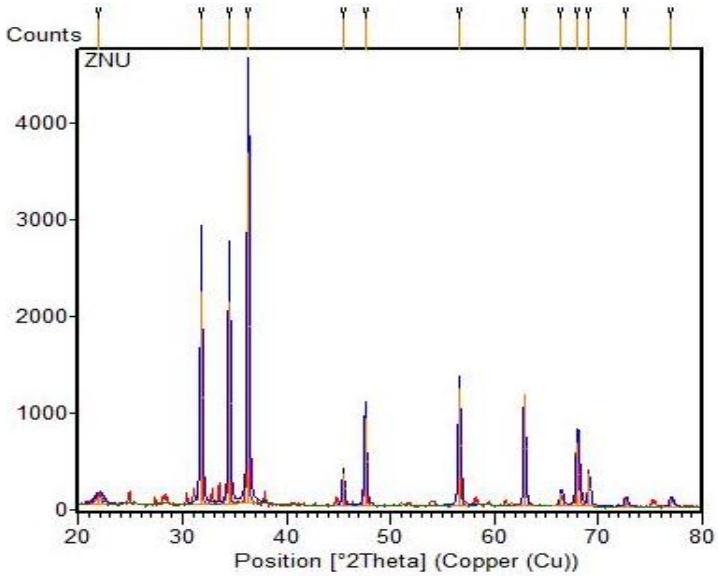

Figure-6 XRD Spectra of zinc nanoparticles using urea– Formaldehyde resin

Table-1 XRD data of zinc nanoparticles usingurea – Formaldehyde resin

S. No.	Pos. [°2Th.]	FWHM Left [°2Th.]	D	DISLOCATION DENSITY	STRAIN
1.	21.97618	0.94464	8.956266	0.012467	0.021228
2.	31.78089	0.1968	43.87832	0.000519	0.003016
3.	34.46995	0.1968	44.18552	0.000512	0.002768
4.	36.29301	0.1968	44.41022	0.000507	0.00262
5.	45.44359	0.1968	45.75163	0.000478	0.002051
6.	47.56873	0.1968	46.11755	0.00047	0.001948
7.	56.61644	0.1968	47.93237	0.000435	0.001594
8.	62.88863	0.15744	61.82922	0.000262	0.001124
9.	66.42747	0.31488	31.52458	0.001006	0.002099
10.	68.00665	0.31488	31.81452	0.000988	0.002037
11.	69.10339	0.15744	64.04529	0.000244	0.000998
12.	72.64902	0.31488	32.73538	0.000933	0.001869
13.	77.03575	0.31488	33.70816	0.00088	0.001726
14.	Average		26.10612	0.001467	0.003468

3. Result and Discussion

The polymer metal complex's FT-IR spectra, as shown in Figure 2, show a band at 3393 cm-1 that is indicative of N-H stretching. Between 2940 cm-1, the C–H asymmetrical and symmetrical stretching caused by the methylene groups may be seen. The aromatic C=C stretching was identified as the cause of the peaks at 1694 cm-1. The Zn-N linkage was responsible for the detected absorption band at 648 cm-1, which further supported the metal-to-metal bonding via the nitrogen of the urea-formaldehyde functional group. The 1H NMR spectrum of the zinc-doped urea-formaldehyde complex is displayed in Figure 3. There were two distinct singlets found in the metal urea-formaldehyde complex. where the peak at 3.3 ppm indicates the solvent's remaining proton signal and the singlet at 2.5 ppm represents the methylene group of the urea formaldehyde polymer. Figures 4(a) and 4(b) show SEM morphology at 10000 and 20000 magnifications, respectively. The presence of a spherical spot on the surface of the nanomaterial composite indicates the presence of metal ions, which become plainly apparent as magnification increases. This graphic accurately depicts the composite's nanostructure. The one-dimensional electron transit on the surface of a composite material is significantly influenced by the spherical metal ion. With energy dispersive X-ray analysis, we can analyze every constituent of the zinc nanoparticles by thermosetting resin. This shows that Zn elements are present, confirming that Zn nanoparticles have formed. The EDX study, which offers quantitative information on the proportions of zinc in nanoparticles, likewise supports this. This might be because the synthesis technique in the current investigation used an open reaction system [22].

X-Ray Diffraction pattern of zinc, nanoparticles are shown in Figure-6. The crystalline size of these nanoparticles have been determined by XRD data using the Scherrer formula [23-24]:

$D = K\lambda / (\beta \cos \theta)$

where D is the crystallites' mean size (in nanometers). The X-ray wave length, denoted by λ, the Bragg angle, B, the full width half maximum (FWHM) of the X-ray diffraction peak, and K, the crystallite form factor (0.9 is a good approximation). Based on peak positions and electron density within the unit cell, the X-RD diffraction pattern offers information on the size and geometry of the unit cell. The size of the urea-formaldehyde doped zinc nanoparticles, as determined by employing table no. 1 data of the peak list, was 26.10 nm.

4. Conclusion

Zinc nanoparticles have been synthesized using an inexpensive, straightforward chemical process. The Zn-polymer complex was precipitated at 50 °C, and then it was calcined at 800 °C to complete

the synthesis. Zn nanoparticles have been verified by XRD, EDS, and SEM, and the successful production of the zinc polymer metal complex has been verified by FT-IR and NMR. SEM verified the spherical shape of zinc nanoparticles. Because of the angle strain between the monomers, XRD measurements verify that the nanoparticles that are generated are crystalline in nature. Our findings unequivocally demonstrate that zinc nanoparticles, which may have further commercial uses, can be synthesized efficiently using the less expensive and environmentally friendly thermal decomposition process.

Availability of data and materials
Not applicable. "Please contact with author for data request''

Competing interest
The authors declare no conflict of interest.

Funding statement
This research did not receive any specific grant from funding agencies in the public, commercial, or not-for-profit sectors.

Acknowledgements-
The authors are also thankful to Manipal University Jaipur, Rajasthan, M.L.S University, Udaipur, Rajasthan, India for providing the characterization facility.

References-

1. Hirano, K.; Asami, M. Phenolic resins-100 years of progress and their future. React. Funct. Polym. 2013, 73, 256–269.
2. Nair, C.P.R. Advances in addition-cure phenolic resins. Prog. Polym. Sci. 2004, 29, 401–498.
3. Lei, Y.; Wu, Q.; Lian, K. Cure kinetics of aqueous phenol-formaldehyde resins used for oriented strandboard
4. manufacturing: Analytical technique. J. Appl. Polym. Sci. 2006, 100, 1642–1650.
5. Rao, C. N. R., Kulkarni, G. U., Thomas, P. J., & Edwards, P. P. (2002). Size-dependent chemistry: properties of nanocrystals. *Chemistry–A European Journal*, *8*(1), 28-35.
6. Grassian, V. H. (2008). When size really matters: size-dependent properties and surface chemistry of metal and metal oxide nanoparticles in gas and liquid phase environments. *The Journal of Physical Chemistry C*, *112*(47), 18303-18313.
7. Ray, P. C. (2010). Size and shape dependent second order nonlinear optical properties of nanomaterials and their application in biological and chemical sensing. *Chemical reviews*, *110*(9), 5332-5365.
8. Mirzaei, H., & Darroudi, M. (2017). Zinc oxide nanoparticles: Biological synthesis and biomedical applications. *Ceramics International*, *43*(1), 907-914.
9. Król, A., Pomastowski, P., Rafińska, K., Railean-Plugaru, V., & Buszewski, B. (2017). Zinc oxide nanoparticles: Synthesis, antiseptic activity and toxicity mechanism. *Advances in colloid and interface science*, *249*, 37-52.
10. Malhotra, S. P. K., & Mandal, T. (2019). Zinc oxide nanostructure and its application as agricultural and industrial material. *Contamin. Agric. Environ. Health Risks Remed*, *1*, 216.
11. Ali, R. N., Naz, H., Li, J., Zhu, X., Liu, P., & Xiang, B. (2018). Band gap engineering of transition metal (Ni/Co) codoped in zinc oxide (ZnO) nanoparticles. *Journal of Alloys and Compounds*, *744*, 90-95.
12. Khan, M. M., Saadah, N. H., Khan, M. E., Harunsani, M. H., Tan, A. L., & Cho, M. H. (2019). Phytogenic synthesis of band gap-narrowed ZnO nanoparticles using the bulb extract of Costus woodsonii. *Bionanoscience*, *9*, 334-344.
13. Imtiazuddin, S. M., Mumtaz, M., & Mallick, K. A. (2012). Pollutants of wastewater characteristics in textile industries. *J Basic App Sci*, *8*, 554-556.

14. Dihom, H. R., Al-Shaibani, M. M., Mohamed, R. M. S. R., Al-Gheethi, A. A., Sharma, A., & Khamidun, M. H. B. (2022). Photocatalytic degradation of disperse azo dyes in textile wastewater using green zinc oxide nanoparticles synthesized in plant extract: A critical review. *Journal of Water Process Engineering*, *47*, 102705.
15. Benelli, G., Caselli, A., & Canale, A. (2017). Nanoparticles for mosquito control: Challenges and constraints. *Journal of King Saud University-Science*, *29*(4), 424-435.
16. Dezfuli, S. M., & Sabzi, M. (2019). Deposition of ceramic nanocomposite coatings by electroplating process: A review of layer-deposition mechanisms and effective parameters on the formation of the coating. *Ceramics International*, *45*(17), 21835-21842.
17. Trieu, V., Schley, B., Natter, H., Kintrup, J., Bulan, A., & Hempelmann, R. (2012). RuO2-based anodes with tailored surface morphology for improved chlorine electro-activity. *Electrochimica acta*, *78*, 188-194.
18. Li, P., He, L., Liu, X., Fan, S., Yuan, Y., Zhang, J., ... & Li, S. (2021). Electro-deposition synthesis of tube-like collagen–chitosan hydrogels and their biological performance. *Biomedical Materials*, *16*(3), 035019.
19. Kumar, R. (2020). $NiCo_2O_4$ nano-/microstructures as high-performance biosensors: a review. *Nano-micro letters*, *12*, 1-52.
20. Beyler, C. L., & Hirschler, M. M. (2002). Thermal decomposition of polymers. *SFPE handbook of fire protection engineering*, *2*(7), 111-131.
21. Witkowski, A., Stec, A. A., & Hull, T. R. (2016). Thermal decomposition of polymeric materials. *SFPE handbook of fire protection engineering*, 167-254.
22. Brault, J., Gendry, M., Grenet, G., Hollinger, G., Desieres, Y., & Benyattou, T. (1998). Role of buffer surface morphology and alloying effects on the properties of InAs nanostructures grown on InP (001). *Applied physics letters*, *73*(20), 2932-2934.
23. Pacella, A., Ballirano, P., & Cametti, G. (2016). Quantitative chemical analysis of erionite fibres using a micro-analytical SEM-EDX method. *European Journal of Mineralogy*, *28*(2), 257-264.
24. Monshi, A., Foroughi, M. R., & Monshi, M. R. (2012). Modified Scherrer equation to estimate more accurately nano-crystallite size using XRD. *World journal of nano science and engineering*, *2*(3), 154-160.
25. Bokuniaeva, A. O., & Vorokh, A. S. (2019, December). Estimation of particle size using the Debye equation and the Scherrer formula for polyphasic TiO2 powder. In *journal of physics: Conference series* (Vol. 1410, No. 1, p. 012057). IOP Publishing.